

Overlap-aware End-to-End Supervised Hierarchical Graph Clustering for Speaker Diarization

Prachi Singh, *Student Member, IEEE*, and Sriram Ganapathy, *Senior Member, IEEE*

Abstract—Speaker diarization, the task of segmenting an audio recording based on speaker identity, constitutes an important speech pre-processing step for several downstream applications. The conventional approach to diarization involves multiple steps of embedding extraction and clustering, which are often optimized in an isolated fashion. While end-to-end diarization systems attempt to learn a single model for the task, they are often cumbersome to train and require large supervised datasets. In this paper, we propose an end-to-end supervised hierarchical clustering algorithm based on graph neural networks (GNN), called End-to-end Supervised Hierarchical Clustering (E-SHARC). The E-SHARC approach uses front-end mel-filterbank features as input and jointly learns an embedding extractor and the GNN clustering module, performing representation learning, metric learning, and clustering with end-to-end optimization. Further, with additional inputs from an external overlap detector, the E-SHARC approach is capable of predicting the speakers in the overlapping speech regions. The experimental evaluation on several benchmark datasets like AMI, VoxConverse and DISPLACE, illustrates that the proposed E-SHARC framework improves significantly over the state-of-art diarization systems.

Index Terms—Speaker diarization, Supervised hierarchical clustering, Graph neural networks, Overlap speech processing.

I. INTRODUCTION

Speaker diarization is the process of automatically identifying and grouping audio segments based on speaker identity in the given recording. It is an important step in many speech-processing applications, such as meeting transcription, broadcast news analysis, speaker verification in conversational audio, call-center applications, etc. The key challenge in the task arises from short speaker turns, noise and reverberation, code-mixing/switching, and overlapping speech. In this paper, we propose a graph neural network-based representation learning and clustering framework for diarization of natural conversational audio.

The widely used efforts in diarization attempt to segment the audio into short segments of 1–2s, which are converted to embeddings, followed by a clustering step. The initial efforts in embedding extraction framework used Gaussian mixture modeling based background models, termed as i-vectors [1]. Recent works in speaker diarization have focused on deep learning-based models such as Time-Delay Neural Networks (TDNN) [2] and residual networks (ResNet) [3]. These models

can effectively extract speaker discriminative features, called x-vectors. The embeddings are used in the clustering step with a pre-defined similarity metric, e.g., Probabilistic Linear Discriminant Analysis (PLDA) scoring [4], [5]. While this approach to diarization allows the use of pre-trained models (like embedding extraction networks and similarity scoring schemes) developed for speaker verification, the framework is highly modular, with each component optimized individually without a multi-speaker diarization loss function.

Metric learning efforts attempt to partially mitigate this issue by learning the similarity metric based on diarization losses [6], [7]. One of the limitations of these approaches is the difficulty in generalizing the learned similarity metric to new speakers and unseen conditions. This has motivated the work on self-supervised metric learning [8], [9], which uses clustering outputs as the pseudo labels for model training. However, even with these efforts, the rest of the embedding extraction and clustering components are modular.

The recent efforts in the development of an end-to-end neural diarization (EEND) system [10], [11] attempt to mitigate the modular issues, where the goal is to perform the entire diarization process in a single neural network. However, these models require large amounts of labeled conversational data for training and involve a large computational overhead. This can be difficult and time-consuming to obtain, and generalization to new unseen domains like multi-lingual or code-mixed settings may be challenging.

To overcome the limitations of metric learning approaches, our prior work (Singh et al. [14]) introduced a supervised hierarchical clustering approach called SHARC, which trains a graph neural network with speaker embeddings as the nodes and similarity scores as the edges. In this paper, we provide an extension of SHARC to incorporate the joint learning of the embedding extractor and the graph neural network. This approach is termed as end-to-end SHARC (E-SHARC). The framework allows the use of any deep learning-based embedding extractors, like ETDNN [27], FTDNN [28], ResNet or ECAPA-TDNN [3] models. The proposed work further tackles the problem of diarization of overlapping speech.

The major contributions of the proposed work are:

- Provide a comprehensive mathematical and algorithmic description of graph-based clustering for speaker diarization task.
- Develop an end-to-end diarization system using supervised graph neural network-based clustering (E-SHARC).
- Introduce an overlap speaker detection approach called as E-SHARC-Overlap to assign multiple speakers for the same audio region.

This work is funded by grants from the British Telecom Research Center (BTIRC) and the Ministry of Information Technology (MEITY) Bhasini program.

The authors are with the Learning and Extraction of Acoustic Patterns (LEAP) lab, Department of Electrical Engineering, Indian Institute of Science, Bangalore 560012, India.

E-mail: prachisingh@iisc.ac.in; sriramg@iisc.ac.in.

- Evaluate the performance on three benchmark datasets to illustrate improvements over state-of-the-art diarization systems.

II. RELATED WORK

A. End-to-end neural diarization

Watanabe et al. [11] introduced a neural processing framework for speaker diarization. The goal is to train a model that predicts the speaker activity labels at each time frame in an audio recording, given the front-end time-frequency features as input. The model also attempts to identify the number of speakers in the conversation using attractor style long short-term memory (LSTM) networks [12]. Due to the difficulty in handling a large number of speakers, speaker similarity-based loss was also added to this framework [13]. In contrast, our work does not require a large amount of supervised conversational training data. Further, the E-SHARC framework can leverage large pre-trained speaker embedding models.

B. Graph clustering algorithms

The task of grouping the vertices of the graph into clusters in such a way that there are more edges within each cluster and relatively few between the clusters is called *graph clustering*. One of the popular methods that originated from graph theory is called spectral clustering [18]. Similarly, another algorithm called path integral clustering (PIC) [8], [19] is a graph-structural agglomerative clustering algorithm where the graph encodes the structure of the feature space. These clustering approaches are unsupervised. In contrast, we propose a supervised graph clustering framework that can be learned using the labeled data. In this work, we describe one of the first efforts in exploring hierarchical graph clustering frameworks for speaker diarization.

C. Overlap detection approaches

Medennikov et al. (2020) [20] proposed target-speaker voice activity detection (TS-VAD) to achieve accurate speaker diarization even under noisy conditions with speaker overlaps. Bullock et al. (2020) [16] proposed the Long Short-Term Memory (LSTM) based architecture for overlap detection. The model in the Pyannotate [17] is trained with hand-crafted features or trainable SincNet features. The model performs 2-class classification (overlapped versus clean speech) using binary cross entropy loss. In contrast, our work utilizes overlapped speech regions in graph clustering to determine the speaker identities.

III. PROPOSED APPROACH

A. Background

Graphs are powerful mathematical structures that represent complex relationships and interactions among entities. Graph algorithms find applications in various areas because of their ability to exploit the structure of data, which can be in any form [21], [22]. Graph frameworks are suitable for diarization problems due to their ability to represent speaker interactions in a conversation naturally.

A graph G can be described by the set of vertices/nodes V and edges E , as $G = (V, E)$. Adjacency matrix ($\mathbf{A} \in \mathcal{R}^{N \times N}$, N - number of nodes) captures connections between nodes. The adjacency matrix can be obtained using similarity scores between data points. Nodes in the graph represent embeddings of individual speakers, and edges capture turn-taking between speakers in the conversation.

A graph neural network (GNN) is an effective tool for analyzing and modeling graphs. The Graph Convolution Network (GCN) [23], the most common variant of GNNs, was used in [24] for semi-supervised training using clustering output as “pseudo-labels”. Speaker diarization can be formulated as a link prediction problem [25] between speaker embeddings of segments from the same recording. The GCN is inherently transductive and does not generalize to unseen nodes. The GraphSAGE [26], another variant of GNN, is a representation learning technique suitable for dynamic graphs. Without the need for retraining, it can predict the embedding of a new node. Therefore, we have explored this variant in the current work.

B. E-SHARC model

The proposed E-SHARC model involves two steps, namely embedding extraction and GNN-based clustering. In this work, we have explored the ETDNN model based embedding extractor.

C. Notations

- $\mathbf{X}_r = \{\mathbf{x}_1, \dots, \mathbf{x}_{N_r}\}$, $\mathbf{x}_i \in \mathbb{R}^D \forall i \in \{1, \dots, N_r\}$ denotes the sequence of N_r segment embeddings for the recording r .
- $m \in \{1, 2, \dots, M\}$ denotes the level (iteration) of hierarchical clustering.
- $G_r^m = (V_r^m, E_r^m)$ is a graph of recording r at level m . V_r^m and E_r^m are the set of vertices and set of edges of the graph, respectively.
- $\mathbf{h}_i^{(m)} = [\tilde{\mathbf{h}}_i^{(m)}; \bar{\mathbf{h}}_i^{(m)}]$ where $\tilde{\mathbf{h}}_i^{(m)}$ is the identity feature of node i at level m . It is the representative feature of the node with the highest density among all nodes of the previous level that were clustered to form i . $\bar{\mathbf{h}}_i^{(m)}$ is the average feature of level m , which is the average of all the identity features from the previous level $m - 1$ (Equation 3). $\mathbf{h}_i^{(0)} = [\mathbf{x}_i; \mathbf{x}_i]$.
- $\mathbb{H}_r^m = \{\mathbf{h}_1^{(m)}, \mathbf{h}_2^{(m)}, \dots, \mathbf{h}_{N_r^m}^{(m)}\} \in \mathcal{R}^{D' \times N_r^m}$ denotes the node features. N_r^m is the number of nodes at level m for recording r and $N_r^0 = N_r$.
- $\mathbf{S}_r^m \in \mathbb{R}^{N_r^m \times N_r^m}$ denotes pairwise similarity score matrix such that $[\mathbf{S}]_{ij} = s(\tilde{\mathbf{h}}_i^{(m)}, \tilde{\mathbf{h}}_j^{(m)})$, the similarity score between identity features of node i and j .
- p_{ij}^m and \hat{p}_{ij}^m denote the ground truth and predicted edge probabilities between node i and j , respectively, at level m . P^m and \hat{P}^m are the ground truth and predicted edge sets, respectively, as shown in Figure 2.
- $\hat{e}_{ij}^m = 2\hat{p}_{ij}^m - 1 \in [-1, 1]$ denotes the edge coefficient or edge weight between node $i \in \{1, \dots, N_r^m\}$ and $j \in J_i^k$, where J_i^k represents the set of k -nn (k -nearest neighbor) nodes of i .

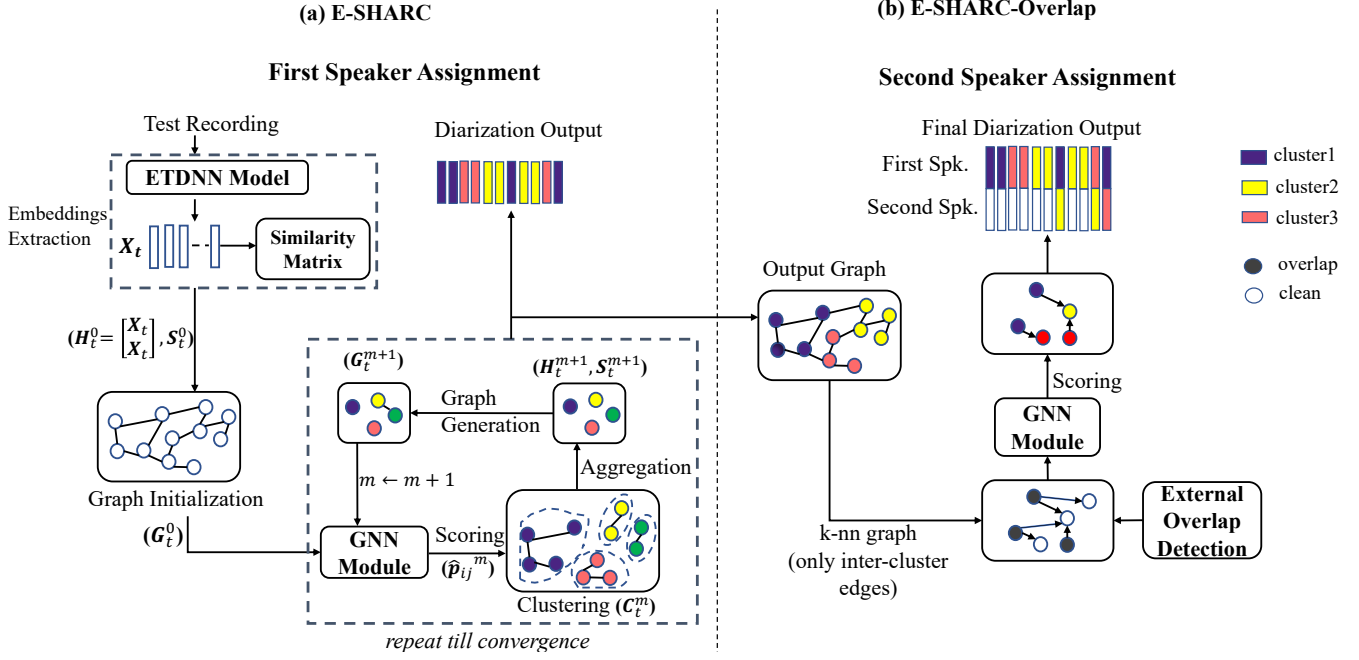


Fig. 1. Block schematic of the E-SHARC algorithm with overlap handling. (a) shows E-SHARC inference containing ETDNN and GNN module for the first speaker assignment. (b) shows E-SHARC-Overlap for the second speaker assignment approach using an external overlap detector and the GNN module.

- $\mathbf{C}_r^m = \{\mathcal{C}_1^m, \dots, \mathcal{C}_{n_c}^m\}$ denotes the set of clusters for level m where each cluster set \mathcal{C}_i^m contains all connected components/nodes without any discontinuity, n_c is the total number of clusters formed. $N_r^{m+1} = n_c$
- Hyper-parameters:
 - k - number of nearest-neighbors
 - τ - threshold on edge probabilities to stop merging.

D. Graph initialization

For both the training and inference steps of the E-SHARC framework, the first step is the creation of a graph based on the input embeddings (x-vectors). The initial graph, termed as the graph at level $m = 0$, $G_t^0 = (V_t^0, E_t^0)$, contains embeddings as the nodes in V_t^0 and k -nearest neighbor of each node based on S_t^0 similarity score matrix that forms the edges in E_t^0 . The pre-trained PLDA model is used to generate similarity scores.

E. Forward pass

Figure 1 (a) shows the block diagram of the inference step. For a test recording t , x-vectors \mathbf{X}_t are extracted to perform hierarchical clustering. The SHARC is performed using a GNN module, which takes the graph as input and generates edge prediction probabilities.

The components of the SHARC algorithm are discussed below.

1) *GNN scoring* : The GNN scoring function Φ is a learnable GNN module designed for supervised clustering. The module jointly predicts node densities and edge probabilities using the input embeddings at each level. Each graph G_t^m , containing source and destination node pairs, is fed to the GNN scoring model. The output of the model is linkage probability \hat{p}_{ij}^m of the nodes v_i^m and $v_j^m \forall i = 1, \dots, N_t^m, j \in J_i^k$.

The edge probabilities are also used to compute node density, which measures how densely the node is connected within the cluster. A node with higher density better represents the cluster than a node with lower density. A node density using predicted edge coefficients is called pseudo density \hat{d}_i^m for node v_i^m and is defined as:

$$\hat{d}_i^m = \frac{1}{k} \sum_{j \in J_i^k} \hat{e}_{ij}^m S_t^m(i, j) \quad (1)$$

The ground truth density d_i^m is obtained using ground truth edge coefficient $e_{ij}^m = 2p_{ij}^m - 1 \in \{-1, 1\}$, where $p_{ij}^m = 1$ if nodes v_i^m and v_j^m belong to the same cluster/speaker, otherwise $p_{ij}^m = 0$.

2) *Clustering*: Clustering is the process of grouping the nodes based on the presence of edge connections. After GNN scoring, clustering is performed hierarchically using the edge probabilities \hat{p}_{ij}^m and the estimated node densities \hat{d}_i^m . At each level of hierarchy m , it creates a candidate edge set $\varepsilon(i)^m$, for the node v_i^m , with edge connection threshold τ as,

$$\varepsilon(i)^m = \{j | (v_i^m, v_j^m) \in E_t^m, \hat{d}_i^m \leq \hat{d}_j^m \text{ and } \hat{p}_{ij}^m \geq \tau\} \quad (2)$$

For any i , if $\varepsilon(i)^m \neq \emptyset$, pick $j = \text{argmax}_{j \in \varepsilon(i)^m} \hat{e}_{ij}^m$ and connect v_i^m and v_j^m . After a full pass over every node, a set of clusters \mathcal{C}_t^m is formed based on connected components.

3) *Feature aggregation*: The cluster nodes at level m are aggregated to form node features of the next level. To obtain node representations for next level \mathbb{H}_t^{m+1} , the clusters \mathcal{C}_t^m and the features \mathbb{H}_t^m are used to compute identity feature $\tilde{h}_i^{(m+1)}$

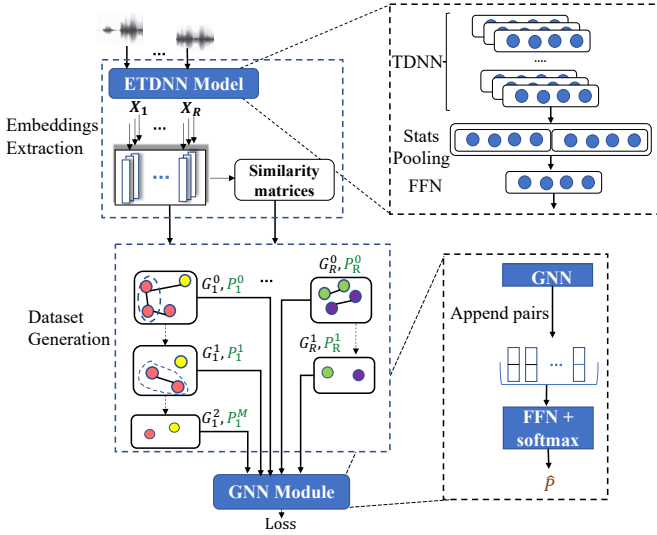


Fig. 2. Block schematic of the E-SHARC training. The ETDNN and GNN modules in blue blocks contain learnable parameters. The GNN module generates edge probabilities and weights used in loss computation.

and average feature $\bar{\mathbf{h}}_i^{(m+1)}$ of each cluster i as,

$$\tilde{\mathbf{h}}_i^{(m+1)} = \tilde{\mathbf{h}}_{z_i}^{(m)}, \quad \bar{\mathbf{h}}_i^{(m+1)} = \frac{1}{|C_i^m|} \sum_{j \in C_i^m} \tilde{\mathbf{h}}_j^{(m)} \quad (3)$$

$$\mathbf{h}_i^{(m+1)} = [\tilde{\mathbf{h}}_i^{(m+1)}; \bar{\mathbf{h}}_i^{(m+1)}]$$

where $z_i = \operatorname{argmax}_{j \in C_i^m} \hat{d}_j^{(m)}$.

4) *Graph generation*: A new graph G_t^{m+1} is constructed for the next level using the node features $\mathbb{H}_t^{(m+1)}$. The edges are formed using S_t^{m+1} which is computed using the identity features $\mathbb{H}_t^{(m+1)}$.

The algorithm repeats until convergence when there are no connected components in the graph, as shown in Figure 1 (a).

F. Model training

E-SHARC training involves learning the embedding extractor and the GNN module (SHARC). During training, multiple graphs are constructed using input features and similarity matrix at different levels of clustering for each of the audio recordings in the training set. The loss combines binary cross entropy loss and mean squared error loss. These losses across all graphs are then accumulated and back-propagated for each batch. The block diagram is shown in Figure 2.

1) *Dataset generation*: For the training set, input graphs $G = \{G_1^0, G_2^0, \dots, G_1^1, \dots, G_R^{M_r}\}$ are constructed at different clustering levels for each recording r . M_r is the maximum number of levels created for r . $E = \{E_1^0, \dots, E_1^{M_1}, \dots, E_R^0, \dots, E_R^{M_R}\}$ and $V = \{V_1^0, \dots, V_1^{M_1}, \dots, V_R^0, \dots, V_R^{M_R}\}$ are the set of all possible edges and nodes, respectively. For each level, clustering is performed based on edge probabilities, allowing only the same speaker embeddings to belong to a single cluster.

2) *SHARC training*: This step uses a pre-trained extended time delay neural network (ETDNN) [27] model for embedding extraction to extract x-vectors. These x-vectors are used to generate the training graphs. In the first step, the weights of the ETDNN module are frozen, and the GNN module weights are learned.

GNN module architecture: The model consists of one GNN layer with $D' = 2048$ units (neurons in a layer). It takes node representations \mathbb{H}^m and their edge connections E_r^m as input and generates latent representations denoted as $\hat{\mathbb{H}}_r^{(m)} \in \mathcal{R}^{D' \times N_r^m}$. Each node v_i associates with a cluster (speaker) label z_i in the training set, allowing the learning of the clustering criterion from the data. The pair of embeddings are concatenated $[\hat{\mathbf{h}}_i; \hat{\mathbf{h}}_j]$ and passed to a fully connected feed-forward network with a size of $\{2D', 1024, 1024, 2\}$ followed by softmax activation to generate edge probability \hat{p}_{ij} . The architecture was selected based on validation experiments.

Loss function: The GNN module is trained using the following loss function.

$$L = L_{conn} + L_{den} \quad (4)$$

where L_{conn} is the pairwise binary cross entropy loss based on edge probabilities across all the possible edges in E given as:

$$L_{conn} = -\frac{1}{|E|} \sum_{(v_i, v_j) \in E} l_{ij} \quad (5)$$

$$l_{ij} = \begin{cases} p_{ij} \log \hat{p}_{ij} + (1 - p_{ij}) \log(1 - \hat{p}_{ij}) & \text{if } d_i \leq d_j \\ 0 & \text{otherwise} \end{cases} \quad (6)$$

Here, $|E|$ represents the total number of edges. L_{den} represents the neighborhood density average loss given by Equation 7. L_{den} represents mean squared error (MSE) loss between ground truth node density d_i and predicted density \hat{d}_i ,

$$L_{den} = \frac{1}{|V|} \sum_{i=1}^{|V|} \|d_i - \hat{d}_i\|_2^2 \quad (7)$$

where $|V|$ is the cardinality of V .

3) *Joint ETDNN and GNN training*: In this step, the GNN module is first initialized using the SHARC trained model. The ETDNN model is also learned along with the GNN module.

ETDNN architecture: The 13-layer ETDNN model follows the architecture described in [27], [29]. The input to the model is 40-D mel-spectrogram features extracted from each segment (1.5s) of the training recording followed by cepstral mean normalization. The model comprises four blocks containing TDNN and a fully connected layer of size 1024D. This is followed by two feed-forward layers containing $\{1024, 2000\}$ units and a segment pooling layer of 4000D concatenating the mean and standard deviation of each segment from the previous layer. This is passed to an affine layer of 512D which is called the x-vector embedding. The model is initialized with a pre-trained model for speaker classification. These x-vectors are used to generate the training graphs as described in the Section III-F1. The loss is back propagated till the TDNN layers.

IV. HANDLING OVERLAPPED SPEECH

We extend the E-SHARC model also to perform GNN-based overlap prediction called E-SHARC-Overlap. Our approach assumes that a maximum of two speakers are present in an overlapping region. We follow a two-pass approach to accurately identify the speakers in the overlapping region. The first pass comprises E-SHARC modeling on the clean segments (single speaker segments). The first speaker, referred to as the parent cluster, is selected for each segment based on the first-pass E-SHARC algorithm. The proposed overlap model is trained using overlapping and clean segments in the second pass. During training, the graph adjacency matrix is generated by connecting the nodes from one cluster to nodes from any other cluster except the parent cluster. This enables the overlap model to identify the second speaker in the overlapping regions. A small percentage of intra-cluster connections (10%) are preserved randomly, enabling contrastive training. The k -nearest neighbors of each node are selected based on the final graph adjacency matrix. The training loss comprises BCE and MSE losses, similar to the original SHARC model (Equation 4).

A. Initialization

The SHARC-Overlap and E-SHARC-Overlap models are initialized with the pre-trained SHARC and E-SHARC models, respectively.

B. Inference

The inference steps comprise first pass - clustering, second pass - overlap detection, and second speaker assignment to generate the final diarization output (Figure 1).

1) *First speaker assignment*: First-pass clustering based on E-SHARC is performed to assign an initial parent cluster and to decide the number of speakers present in a recording, as described in Section III-E. The input x-vectors are the average of the pre-trained x-vectors and the E-SHARC x-vectors.

2) *Second/Overlap speaker assignment*: The overlap or second speaker assignment is done using the E-SHARC-Overlap model. The pyannote overlap detector [16], [17] is used to identify regions containing overlapped speech. A new graph is created using overlapping nodes and their k -nn after removing the within-cluster connections. Then, for each node, top k' ($k' \leq k$) neighbors are selected based on edge probabilities from the E-SHARC-Overlap model. The dominant cluster identity of the neighbors is assigned as the second speaker for the node.

V. EXPERIMENTS

A. Datasets

- **The AMI dataset**: The official speech recognition partition of the AMI dataset [30] comprises training, development (dev), and evaluation (eval) sets consisting of 136, 18, and 16 recordings sampled at 16kHz, respectively. The single-distant microphone (SDM) condition of the AMI dataset is used for experiments. It contains single-channel microphone recordings. The AMI train set contains 75 hrs of labeled

speech. The number of speakers and the duration of each recording ranges from 3-5 and 20-60 mins, respectively.

- **The Voxconverse dataset**: It is an audio-visual diarization dataset [31] consisting of multispeaker human speech recordings extracted from YouTube videos. It is divided into a development (dev) set and an evaluation (eval) set consisting of 216 and 232 recordings, respectively. The duration of a recording ranges from 22-1200 s. The number of speakers per recording varies from 1-21.

As the Voxconverse dataset does not have a train set, the dataset used for training is simulated using Voxceleb 1 and 2 [32], [33] and Librispeech [34] following the recipe mentioned in [35]. We simulated 5000 mixtures containing 2-5 speakers with duration ranging from 150-440 s. This generates 1000 hrs of data with 6,023 speakers.

- **The DISPLACE challenge dataset**: The DISPLACE 2023 [36] dataset released as part of the challenge comprises single-channel far-field natural multilingual, multi-speaker conversational speech recordings. The development (dev) and evaluation phase 2 (eval) sets contain 27 recordings (15.5 hours) and 29 recordings (16 hours), respectively. The speakers in the dev and eval sets are mutually exclusive. The dataset contains conversations in Hindi, Kannada, Bengali, Malayalam, Telugu, Tamil, and Indian English. In each recording, the number of speakers varies from 3-5, and the number of languages varies from 1-3.

B. Baseline system

The baseline method is an x-vector clustering-based approach described in [9], [37]. First, the recording is divided into 1.5s segments with 0.75s shift. The 40D mel-spectrogram features are computed from each segment which is passed to the ETDNN model [27] to extract 512D x-vectors. The ETDNN model is trained on the VoxCeleb1 [32] and VoxCeleb2 [33] datasets, for the speaker identification task, to discriminate among the 7,146 speakers. The whitening transform, length normalization, and recording level PCA (dimension=30) are applied to the x-vectors as pre-processing steps. These embeddings are used to compute the PLDA similarity score matrix and clustered to generate speaker labels for each segment. The PLDA model is trained using the x-vectors.

For the baseline system, we have used the two most popular clustering approaches - Agglomerative Hierarchical Clustering (AHC) [38] and Spectral Clustering (SC) [18]. The PLDA similarity scores are used directly to perform AHC. For SC, we convert the PLDA scores s to $s' \in [0, 1]$ by applying sigmoid with temperature parameter $\tau = 0.1$ (best value obtained from experimentation) as: $s' = \frac{1}{1 + \exp(-s/\tau)}$. This helps to improve the performance without other preprocessing steps usually followed in previous implementations [6].

C. Implementation details

1) *Optimizer* : The SHARC model is trained with a Stochastic Gradient Descent (SGD) optimizer with a learning rate $lr=0.01$ (for Voxconverse) and $lr=1e-3$ (for AMI) for 500 epochs. Similarly, the E-SHARC is also trained with an SGD

TABLE I
CHOICE OF HYPER-PARAMETERS (HP) FOR TRAIN, DEV, EVAL SPLIT OF AMI AND VOXCONVERSE DATASETS.

Model	HP	AMI			Voxconverse		
		Train	Dev	Eval	Train	Dev	Eval
SHARC	k	60	60	60	60	30	30
SHARC	τ	-	0.0	0.0	-	0.5	0.8
E-SHARC	k	30	50	50	60	30	30
E-SHARC	τ	-	0.0	0.0	-	0.9	0.8

TABLE II
PERFORMANCE COMPARISON BASED ON CLUSTER PURITY AND COVERAGE FOR VOXCONVERSE DATASET. SC STANDS FOR SPECTRAL CLUSTERING.

Method	Cluster Purity	Cluster Coverage
Baseline with AHC	93.5	89.5
Baseline with SC	92.0	92.3
SHARC	93.0	92.4
E-SHARC	93.0	92.9

optimizer. In this case, the learning rate is $1e-6$ for the ETDNN model and $1e-3$ for the GNN module; the model is trained for 20 epochs. SHARC-Overlap is initialized with SHARC model weights and trained with $lr=1e-3$ for 100 epochs. E-SHARC-Overlap is initialized with E-SHARC model weights and trained for five epochs.

2) *Adjacency matrix*: The graph adjacency matrix of each recording is obtained using a similarity matrix with k highest similarities in each row. At each level of the hierarchy, the x -vectors, also called the node identity features, are passed to the PLDA model to generate the similarity score matrix.

VI. RESULTS

The performance of the system is measured based on Diarization Error Rate (DER) [39]. It is the sum of false alarm, miss rate, and speaker confusion error. The implementation is based on *dscore toolkit*¹. We have used ground truth speech activity decisions for evaluating AMI and Voxconverse datasets.

We also evaluate our trained model on the DISPLACE challenge dataset. As per challenge guidelines, we have used the DISPLACE challenge baseline SAD model. The model is based on TDNN architecture [36], [37] with speech and non-speech classification. The Voxconverse E-SHARC model is also used for DISPLACE evaluations as the DISPLACE dataset does not contain a training partition.

A. Comparison with the baseline systems

The best values of hyper-parameters k and τ are obtained based on DER on the dev set, applied on the eval set, and vice versa for all the datasets. Table I shows the values of hyper-parameters used for the AMI and Voxconverse experiments.

Table II reports the performance based on the cluster purity and coverage on Voxconverse dev set using pyannote-metric [40]. **Cluster purity** is defined as the percentage of segments from predicted speakers belonging to the corresponding

speaker in the ground truth. **Cluster coverage** is defined as the percentage of segments from the ground truth speaker covered by the predicted speaker. From the table, it can be observed that the baseline with AHC has high purity but low coverage. However, the baseline with spectral clustering (SC) has lower purity but higher coverage. In our proposed approach, both the purity and the coverage are high, indicating that supervised clustering can achieve the best of both worlds.

Table III shows the false alarm (FA), miss, and confusion error along with the overall DER metric of baseline AHC, SC approaches, and the proposed SHARC/E-SHARC models with and without overlap assignment for three different datasets: AMI Single Distant Microphone (SDM), Voxconverse and DISPLACE challenge datasets. From Table III, it can be observed that SHARC and E-SHARC perform significantly better than AHC and SC baselines on all the datasets. E-SHARC achieves 11% and 13% relative improvements over the best baseline on AMI and Voxconverse datasets, respectively.

To fairly compare the performance of SHARC-Overlap and E-SHARC-Overlap with the baseline clustering approaches, we have also integrated the overlap assignment for AHC and SC, which is similar to the E-SHARC-Overlap approach.

Baseline overlap assignment (AHC/SC+Overlap): The first pass clustering (AHC/SC) is performed using the PLDA similarity scores matrix to generate the parent speaker labels for each x -vector. The pyannote overlap detector is used to select the x -vector segments containing overlaps. The within-cluster similarity scores are set to the lowest value for these overlapping segments in the matrix. Then, the top k' similarity scores of each overlapping x -vector are selected for the second pass clustering. The parent speaker labels are assigned for these top k' scores. The mode of the k' parent speaker labels is the second speaker assigned to the overlapping regions. The value of k' is selected as 30 based on validation experiments for SHARC-Overlap and E-SHARC-Overlap.

From Table III, it can be observed that adding overlap assignment to AHC and SC improves the DER performance. Further improvements are obtained with the proposed SHARC-Overlap and E-SHARC-Overlap approaches. We achieve 11.6%, 16.8%, and 25.3% relative improvements for AMI, Voxconverse, and DISPLACE, respectively, over the best baseline system.

Table IV shows the results of baseline and proposed approaches with VBx resegmentation [41]. The VBx is initialized with the corresponding clustering output followed by a resegmentation step using the HMM-PLDA model. It can be observed that VBx segmentation improves performance as it helps refine the speaker boundaries based on temporal information. However, SHARC/E-SHARC initialization requires only 1-2 VBx iterations for convergence to the lowest DER. After the VBx iterations, the second speaker is predicted for the overlapping regions based on the second-highest posterior probability. The E-SHARC-Overlap + VBx achieves the lowest DER for all the datasets, resulting in 9.4%, 4.3%, and 12.6% relative improvements for AMI, Voxconverse, and DISPLACE, respectively over the best baseline system.

¹<https://github.com/nryant/dscore>

TABLE III
DER (%) COMPARISON ON THE AMI, VOXCONVERSE, AND DISPLACE DATASETS WITH THE BASELINE METHODS CONSIDERING OVERLAPS AND WITHOUT TOLERANCE COLLAR.

System	AMI Eval				Voxconverse Eval				DISPLACE Eval			
	FA	Miss	Conf.	DER	FA	Miss	Conf.	DER	FA	Miss	Conf.	DER
AHC	0.0	15.6	13.9	29.51	0.0	3.1	10.31	13.41	3.1	22.4	15.0	40.60
AHC+Overlap	0.7	11.6	14.37	26.67	0.8	1.6	9.65	12.05	3.8	21.0	15.67	40.47
SC	0.0	15.6	6.7	22.29	0.0	3.1	10.9	14.02	3.1	22.4	15.3	40.84
SC+Overlap	0.7	11.6	8.06	20.36	0.8	1.6	11.33	13.73	3.8	21.0	15.85	40.65
SHARC	0.0	15.6	5.7	21.27	0.0	3.1	10.2	13.29	3.1	22.4	7.47	33.07
SHARC-Overlap	0.7	11.6	7.2	19.50	0.8	1.6	10.16	12.56	3.8	21.0	7.9	32.73
E-SHARC	0.0	15.6	4.3	19.83	0.0	3.1	8.5	11.68	3.1	22.4	7.33	32.93
E-SHARC-Overlap	0.7	11.6	5.69	17.99	0.8	1.6	9.02	11.42	3.8	21.0	7.65	32.45

TABLE IV
DER (%) COMPARISON ON THE AMI, VOXCONVERSE, AND DISPLACE DATASETS WITH THE BASELINE METHODS AFTER VBx RESEGMENTATION. CONSIDERING OVERLAPS AND WITHOUT TOLERANCE COLLAR.

System	AMI Eval				Voxconverse Eval				DISPLACE Eval			
	FA	Miss	Conf.	DER	FA	Miss	Conf.	DER	FA	Miss	Conf.	DER
AHC+VBx	0.0	15.6	11.9	27.43	0.0	3.1	8.6	11.72	3.1	22.4	11.15	36.75
AHC+Overlap+VBx	0.7	11.6	11.63	23.93	0.8	1.6	8.45	10.85	3.8	21.0	12.26	37.06
SC+VBx	0.0	15.6	5.3	20.90	0.0	3.1	7.6	10.71	3.1	22.4	10.38	35.98
SC+Overlap+VBx	0.7	11.6	6.7	19.00	0.8	1.6	8.16	10.56	3.8	21.0	11.12	35.92
SHARC + VBx	0.0	15.6	4.8	20.34	0.0	3.1	7.2	10.30	3.1	22.4	6.29	31.89
SHARC-Overlap + VBx	0.7	11.6	6.26	18.56	0.8	1.6	7.8	10.19	3.8	21.0	6.77	31.57
E-SHARC+VBx	0.0	15.6	3.68	19.16	0.0	3.1	7.05	10.15	3.1	22.4	6.8	32.61
E-SHARC-Overlap + VBx	0.7	11.6	4.91	17.21	0.8	1.6	7.7	10.11	3.8	21.0	6.6	31.40

TABLE V
DER (% , WITH OVERLAP + WITHOUT COLLAR) AND DER* (% , WITHOUT OVERLAP + WITH 0.25s COLLAR) COMPARISON WITH STATE-OF-THE-ART ON AMI SDM EVAL, VOXCONVERSE EVAL, AND DISPLACE EVAL(PHASE 2) DATASETS.

AMI SDM System	DER	DER*
Pyannote [42]	29.1	-
x-vec+AHC+VBx [41]	27.4	12.6
SelfSup-PLDA-PIC +VBx [9]	23.8	5.5
Raj et al. [43]	23.7	-
Plaquet et al. [44]	22.9	-
GAE-based+ SC [45]	-	5.5
GADEC-based [45]	-	4.2
E-SHARC (proposed)	19.83	2.9
E-SHARC-Ovp +VBx (prop.)	17.2	2.6
Voxconverse System		
Pyannote [42]	11.9	-
Plaquet et al. [44]	10.4	-
GAE-based+ SC [45]	-	8.0
GADEC-based [45]	-	7.6
E-SHARC (prop.)	11.68	7.6
E-SHARC-Ovp +VBx (proposed)	10.1	6.3
DISPLACE System		
DISPLACE Baseline [36], [46]	32.2	14.6
E-SHARC-Ovp +VBx (prop.) + Baseline SAD	31.4	13.0
Winning system [46]	27.8	7.3

B. Comparison with the other published works

Table V compares the proposed approach with state-of-the-art approaches for AMI, Voxconverse, and DISPLACE datasets. Pyannote [42] is the end-to-end pyannote model with overlap detection modules. Raj et al. [43], and Plaquet et al. [44] explore the recent end-to-end models for diariza-

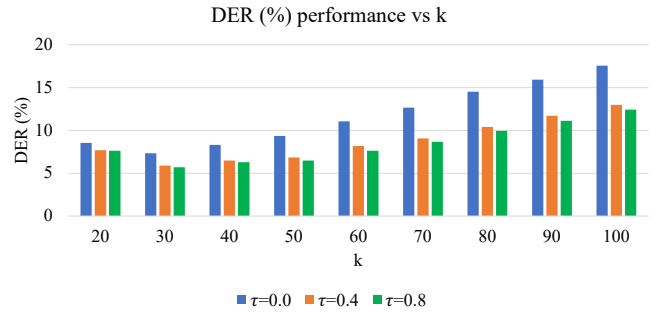


Fig. 3. Plot comparing DER performance for k ranging from 20-100 and $\tau \in \{0.0, 0.4, 0.8\}$ for Voxconverse dev set.

tion. The work reported in [45] proposed Graph Attention-Based Deep Embedded Clustering (GADEC), which performs graph attention-based clustering using multi-objective training. It also shows the results of the Graph attentional encoder (GAE) based approach for metric learning followed by spectral clustering. Our E-SHARC-Ovp + VBx outperforms the state-of-the-art results for AMI SDM and Voxconverse systems. In the case of DISPLACE, the winning system investigated different SAD and model combination strategies, while the proposed system was trained on out-of-set (Voxceleb) data.

VII. ABLATION STUDIES

A. Choice of hyper-parameters

SHARC parameters (k, τ): A high value of k while training allows to capture more edges in the graph and improves the

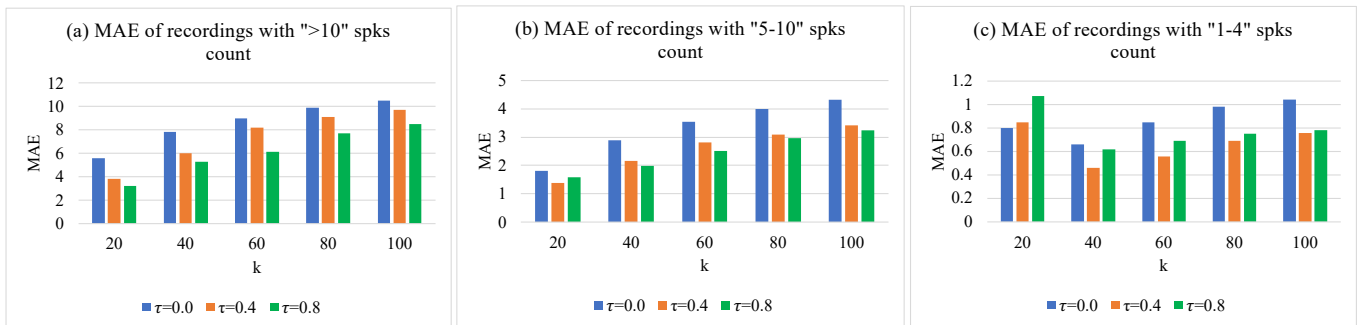


Fig. 4. Plot comparing mean absolute error (MAE) for speaker counting task with k ranging from 20-100 and $\tau \in \{0.0, 0.4, 0.8\}$ for Voxconverse dev.

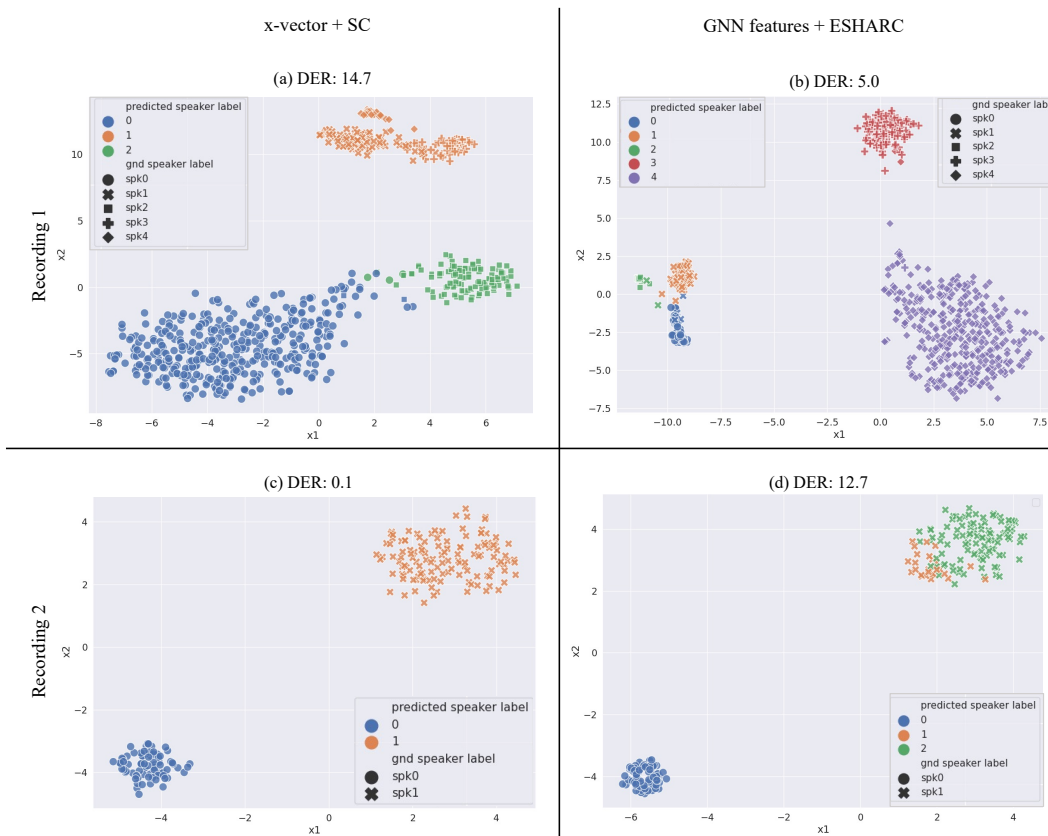


Fig. 5. 2D t-SNE plot to compare x-vectors and GNN embeddings for two different recordings from Voxconverse dev set. The first column shows the x-vectors with SC labels in different colors, and the second column shows GNN features with ESHARC labels in different colors. Ground truth labels are represented as different shapes. In both cases, the proposed E-SHARC yields representations with better separability. However, the DER deteriorated due to early stopping in Recording 2.

model predictions. However, a higher value of k while testing results in fewer levels and clusters. Therefore, the choice of k is also dependent on the average number of speakers present in a recording. The parameter τ (edge prediction probability threshold) sets the minimum required probability to allow the edge connection between nodes. Therefore, a higher value leads to fewer connections, generating a higher number of clusters.

Figure 3 shows the impact of different values of k and τ on DER on the Voxconverse dev set. As k increases, the DER increases as higher k generates fewer speakers. On the other

hand, the DER is higher for a smaller value of τ ($\tau < 0.2$). The best values of k and τ are 30 and 0.8.

B. Speaker counting task

We also perform the speaker counting task evaluation using the proposed model. Figure 4 shows the performance of the speaker counting task for the Voxconverse dataset. It shows the impact of k and τ on the mean absolute error (MAE) between the ground truth number of speakers and the predicted number of speakers. The figure is divided into three categories of recordings based on the number of speakers present. Plot

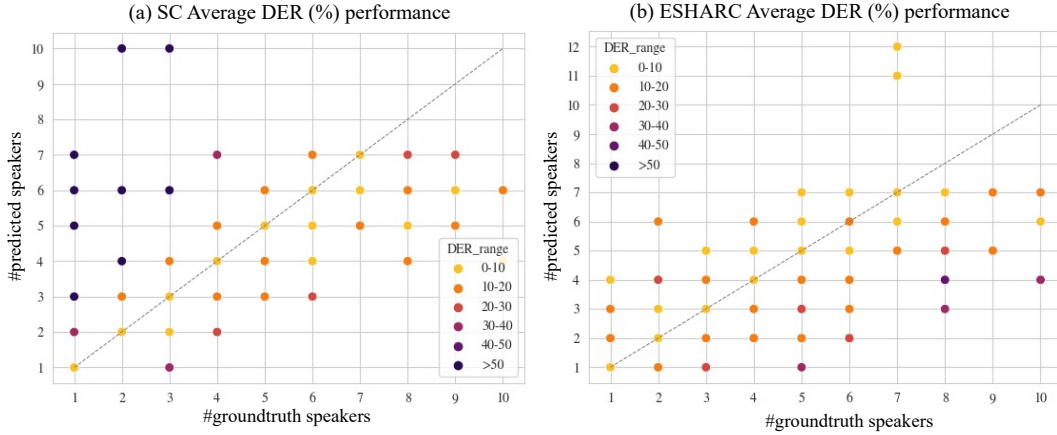


Fig. 6. 2D scatter plot showing no. of ground truth speakers vs no. of predicted speakers using (a) SC and (b) ESHARC on Voxconverse dev set. The different colors represent different ranges of average DER (%) for a pair of (#ground speaker, #predicted speakers).

(a) shows the MAE for recordings with a higher number of speakers (> 10). As k increases, MAE increases, and as τ increases, MAE reduces. Plot (b) shows the MAE for recordings containing a moderate number of speakers (5–10). Finally, plot (c) shows the MAE for recordings containing a small number of speakers (1–4). In this case, MAE is relatively low across different k and τ .

C. Representation visualization

Figure 5 shows the t-SNE plots for two recordings (two rows) from Voxconverse dev set for baseline and the proposed ESHARC approach. The first column shows a t-SNE plot of x-vectors with SC, and the second column shows GNN features with ESHARC. Recording 1 contains five speakers represented by different shapes. The SC predicts only three speakers out of five, as shown in different colors. However, E-SHARC can form five different clusters and provide a lower DER. It can also be observed that the within-cluster covariance is lower for the GNN features compared to x-vectors. For recording 2, the SC can predict the correct number of speakers. On the other hand, E-SHARC splits spk1 from ground truth into two different speakers shown in different colors. Although the features are well separated in terms of speaker clusters, the stopping criterion has resulted in early stopping.

Figure 6 shows a 2D scatter plot comparing the performance of SC and ESHARC in terms of the predicted number of speakers on Voxconverse dev. The color represents different ranges of filewise DER for the particular pair of (#groundtruth speakers, #predicted speakers). It can be observed that, for files with a lower number of speakers (< 4), the model predicts a very high number of speakers, which leads to very high DERs (> 50) for SC (Figure 6 (a)). On the other side, Figure 6 (b) shows the scatter plot for the E-SHARC model. The E-SHARC model can correctly predict speakers for files with fewer speakers in the ground truth, which results in lower DER (0-10). The E-SHARC predicts fewer speakers than the ground truth for other files, but it does not affect the DER performance adversely.

VIII. CONCLUSION

This paper proposes a novel end-to-end supervised hierarchical neural graph clustering approach for speaker diarization. The proposed approach involves supervised graph model training with a clustering-based loss. This model, called E-SHARC, performs hierarchical clustering using a GNN model by minimizing intra-speaker distances and maximizing inter-speaker distances. The model is further extended to perform overlapped speaker prediction. This enables the prediction and assignment of multiple speakers in the overlapped speech regions, further improving the diarization performance. We also showed the effectiveness of the proposed approach on a challenging code-mixed DISPLACE dataset.

ACKNOWLEDGMENTS

The authors would like to thank Amrit Kaul for helping in the initial experiments. The authors would like to thank Michael Free, Rohit Singh, and Shakti Srivastava from BT Research for their valuable input. The authors also thank Hervé Bredin for providing pretrained pyannote SAD and Overlap detection models.

REFERENCES

- [1] N. Dehak, P. J. Kenny, R. Dehak, P. Dumouchel, and P. Ouellet, "Front-end factor analysis for speaker verification," *IEEE Transactions on Audio, Speech, and Language Processing*, vol. 19, no. 4, pp. 788–798, 2010.
- [2] D. Snyder, D. Garcia-Romero, G. Sell, D. Povey, and S. Khudanpur, "X-vectors: Robust DNN embeddings for speaker recognition," in *IEEE ICASSP*, 2018, pp. 5329–5333.
- [3] N. Dawalatabad, M. Ravanelli, F. Grondin, J. Thienpondt, B. Desplanques, and H. Na, "ECAPA-TDNN Embeddings for Speaker Diarization," in *Interspeech*, 2021, pp. 3560–3564.
- [4] S. Ioffe, "Probabilistic linear discriminant analysis," in *European Conference on Computer Vision*. Springer, 2006, pp. 531–542.
- [5] G. Sell and D. Garcia-Romero, "Speaker diarization with PLDA i-vector scoring and unsupervised calibration," in *IEEE Spoken Language Technology Workshop (SLT)*, 2014, pp. 413–417.
- [6] Q. Lin, R. Yin, M. Li, H. Bredin, and C. Barras, "LSTM Based Similarity Measurement with Spectral Clustering for Speaker Diarization," in *Proc. Interspeech*, 2019, pp. 366–370.
- [7] V. S. Narayanaswamy, J. J. Thiagarajan, H. Song, and A. Spanias, "Designing an effective metric learning pipeline for speaker diarization," in *IEEE ICASSP*, 2019, pp. 5806–5810.

- [8] P. Singh and S. Ganapathy, "Self-supervised representation learning with path integral clustering for speaker diarization," *IEEE/ACM Transactions on Audio, Speech, and Language Processing*, vol. 29, pp. 1639–1649, 2021. [Online]. Available: <http://dx.doi.org/10.1109/TASLP.2021.3075100>
- [9] —, "Self-supervised metric learning with graph clustering for speaker diarization," in *IEEE ASRU*, 2021, pp. 90–97.
- [10] Y. Fujita, S. Watanabe, S. Horiguchi, Y. Xue, J. Shi, and K. Nagamatsu, "Neural speaker diarization with speaker-wise chain rule," *arXiv preprint arXiv:2006.01796*, 2020.
- [11] S. Horiguchi, Y. Fujita, S. Watanabe, Y. Xue, and K. Nagamatsu, "End-to-End Speaker Diarization for an Unknown Number of Speakers with Encoder-Decoder Based Attractors," in *Interspeech*, 2020.
- [12] —, "End-to-end speaker diarization for an unknown number of speakers with encoder-decoder based attractors," *arXiv preprint arXiv:2005.09921*, 2020.
- [13] S. Horiguchi, S. Watanabe, P. García, Y. Xue, Y. Takashima, and Y. Kawaguchi, "Towards neural diarization for unlimited numbers of speakers using global and local attractors," in *IEEE ASRU*, 2021, pp. 98–105.
- [14] P. Singh, A. Kaul, and S. Ganapathy, "Supervised hierarchical clustering using graph neural networks for speaker diarization," in *International Conference on Acoustics, Speech and Signal Processing (ICASSP)*. IEEE, 2023, pp. 1–5.
- [15] Y. Xing, T. He, T. Xiao, Y. Wang, Y. Xiong, W. Xia, D. Wipf, Z. Zhang, and S. Soatto, "Learning hierarchical graph neural networks for image clustering," in *Proc. IEEE ICCV*, 2021, pp. 3467–3477.
- [16] L. Bullock, H. Bredin, and L. P. Garcia-Perera, "Overlap-aware diarization: Resegmentation using neural end-to-end overlapped speech detection," in *IEEE International Conference on Acoustics, Speech and Signal Processing (ICASSP)*, 2020, pp. 7114–7118.
- [17] H. Bredin, R. Yin, J. M. Coria, G. Gelly, P. Korshunov, M. Lavechin, D. Fustes, H. Titeux, W. Bouaziz, and M.-P. Gill, "pyannote.audio: neural building blocks for speaker diarization," in *ICASSP 2020, IEEE International Conference on Acoustics, Speech, and Signal Processing*, Barcelona, Spain, May 2020.
- [18] A. Ng, M. Jordan, and Y. Weiss, "On spectral clustering: Analysis and an algorithm," *Advances in neural information processing systems*, vol. 14, 2001.
- [19] W. Zhang, D. Zhao, and X. Wang, "Agglomerative clustering via maximum incremental path integral," *Pattern Recognition*, vol. 46, no. 11, pp. 3056–3065, 2013. [Online]. Available: <https://www.sciencedirect.com/science/article/pii/S0031320313001830>
- [20] I. Medennikov, M. Korenevsky, T. Prisyach, Y. Khokhlov, M. Korenevskaya, I. Sorokin, T. Timofeeva, A. Mitrofanov, A. Andrusenko, I. Podluzhny, A. Laptev, and A. Romanenko, "Target-Speaker Voice Activity Detection: A Novel Approach for Multi-Speaker Diarization in a Dinner Party Scenario," in *Proc. Interspeech 2020*, 2020, pp. 274–278. [Online]. Available: <http://dx.doi.org/10.21437/Interspeech.2020-1602>
- [21] A. Bondy and U. Murty, *Graph Theory with Applications*. Wiley, 1991. [Online]. Available: <https://books.google.co.in/books?id=7EWKkgEACAAJ>
- [22] A. Majeed and I. Rauf, "Graph theory: A comprehensive survey about graph theory applications in computer science and social networks," *Inventions*, vol. 5, no. 1, p. 10, 2020.
- [23] T. N. Kipf and M. Welling, "Semi-supervised classification with graph convolutional networks," *arXiv preprint arXiv:1609.02907*, 2016.
- [24] F. Tong *et al.*, "Graph convolutional network based semi-supervised learning on multi-speaker meeting data," in *IEEE ICASSP*, 2022, pp. 6622–6626.
- [25] J. Wang *et al.*, "Speaker diarization with session-level speaker embedding refinement using graph neural networks," in *IEEE ICASSP*, 2020, pp. 7109–7113.
- [26] W. Hamilton, Z. Ying, and J. Leskovec, "Inductive representation learning on large graphs," *Advances in neural information processing systems*, vol. 30, 2017.
- [27] D. Snyder, D. Garcia-Romero, G. Sell, A. McCree, D. Povey, and S. Khudanpur, "Speaker recognition for multi-speaker conversations using x-vectors," in *IEEE ICASSP*, 2019, pp. 5796–5800.
- [28] D. Povey, G. Cheng, Y. Wang, K. Li, H. Xu, M. Yarmohammadi, and S. Khudanpur, "Semi-Orthogonal Low-Rank Matrix Factorization for Deep Neural Networks," in *Proc. Interspeech 2018*, 2018, pp. 3743–3747.
- [29] H. Zeinali *et al.*, "BUT system description to voxceleb speaker recognition challenge 2019," *arXiv preprint arXiv:1910.12592*, 2019.
- [30] I. McCowan, J. Carletta, W. Kraaij, S. Ashby, S. Bourban, M. Flynn, M. Guillemot, T. Hain, J. Kadlec, V. Karaiskos *et al.*, "The AMI meeting corpus," in *International Conference on Methods and Techniques in Behavioral Research*, 2005, pp. 137–140.
- [31] J. S. Chung *et al.*, "Spot the Conversation: Speaker Diarisation in the Wild," in *Proc. Interspeech 2020*, 2020, pp. 299–303.
- [32] A. Nagrani, J. S. Chung, and A. Zisserman, "Voxceleb: A large-scale speaker identification dataset," *Proc. of Interspeech*, pp. 2616–2620, 2017.
- [33] J. S. Chung, A. Nagrani, and A. Zisserman, "Voxceleb2: Deep speaker recognition," in *Proc. of Interspeech*, 2018, pp. 1086–1090.
- [34] V. Panayotov *et al.*, "Librispeech: an asr corpus based on public domain audio books," in *IEEE ICASSP*, 2015, pp. 5206–5210.
- [35] Y. Fujita *et al.*, "End-to-End Neural Speaker Diarization with Self-attention," in *ASRU*, 2019, pp. 296–303.
- [36] S. Baghel, S. Ramoji, P. Singh, S. Jain, P. R. Chowdhuri, K. Kulkarni, S. Padhi, D. Vijayasanen, S. Ganapathy *et al.*, "Displace challenge: Diarization of speaker and language in conversational environments," *arXiv preprint arXiv:2303.00830*, 2023.
- [37] N. Ryant *et al.*, "The Third DIHARD Diarization Challenge," in *Proc. Interspeech*, 2021, pp. 3570–3574.
- [38] W. H. E. Day and H. Edelsbrunner, "Efficient algorithms for agglomerative hierarchical clustering methods," *Journal of Classification*, vol. 1, pp. 7–24, 1984.
- [39] J. G. Fiscus, J. Ajot, M. Michel, and J. S. Garofolo, "The rich transcription 2006 spring meeting recognition evaluation," in *Machine Learning for Multimodal Interaction: Third International Workshop, MLMI 2006, Bethesda, MD, USA, May 1-4, 2006, Revised Selected Papers 3*. Springer, 2006, pp. 309–322.
- [40] H. Bredin, "pyannote.metrics: a toolkit for reproducible evaluation, diagnostic, and error analysis of speaker diarization systems," in *Interspeech 2017, 18th Annual Conference of the International Speech Communication Association*, Stockholm, Sweden, August 2017. [Online]. Available: <http://pyannote.github.io/pyannote-metrics>
- [41] F. Landini *et al.*, "Bayesian HMM clustering of x-vector sequences (VBx) in speaker diarization: theory, implementation and analysis on standard tasks," *arXiv preprint arXiv:2012.14952*, 2020.
- [42] H. Bredin and A. Laurent, "End-To-End Speaker Segmentation for Overlap-Aware Resegmentation," in *Proc. Interspeech 2021*, 2021, pp. 3111–3115.
- [43] D. Raj, D. Povey, and S. Khudanpur, "Gpu-accelerated guided source separation for meeting transcription," *arXiv preprint arXiv:2212.05271*, 2022.
- [44] A. Plaquet and H. Bredin, "Powerset multi-class cross entropy loss for neural speaker diarization," in *Proc. Interspeech 2023*, 2023, pp. 3222–3226.
- [45] Y. Wei, H. Guo, Z. Ge, and Z. Yang, "Graph attention-based deep embedded clustering for speaker diarization," *Speech Communication*, vol. 155, p. 102991, 2023.
- [46] S. Baghel, S. Ramoji, S. Jain, P. R. Chowdhuri, P. Singh, D. Vijayasanen, and S. Ganapathy, "Summary of the displace challenge 2023—diarization of speaker and language in conversational environments," *arXiv preprint arXiv:2311.12564*, 2023.